


Cite this: *RSC Adv.*, 2025, 15, 42507

Received 21st September 2025  
Accepted 28th October 2025

DOI: 10.1039/d5ra07147j

rsc.li/rsc-advances

# Fin effect enables self-controlled growth of nanowires

Beom Seok Kim,<sup>ID</sup>\*<sup>a</sup> Sangwoo Shin<sup>ID</sup><sup>b</sup> and Hyung Hee Cho<sup>ID</sup>\*<sup>c</sup>

Poor length uniformity in nanowires synthesized by template-assisted electrodeposition remains a bottleneck to the development of nanowire-based energy and electronic devices. This fabrication method is inherently unstable, often amplifying non-uniform growth and making precise control difficult. In this work, we investigate how introducing a temperature gradient along individual Bi nanowires enables self-controlled growth that suppresses such instability and improves length uniformity. The temperature difference at the nanowire tips, induced by the fin effect, regulates the local growth rate of each nanowire, allowing the system to equilibrate toward uniform lengths. This approach not only enhances the feasibility of nanowire-based technologies but also provides fundamental insights into self-regulating growth mechanisms, offering new opportunities in materials science.

## 1. Introduction

Nanowires are regarded as promising building blocks for next-generation electronic and energy technologies, and their development remains a central focus of nanoscience research.<sup>1–4</sup> Synthesizing nanowires for these applications requires scalability, simplicity, and selectivity. In this context, the template-assisted electrodeposition method offers distinct advantages over other methods by meeting these criteria.<sup>5,6</sup> In template-assisted electrodeposition, a porous scaffold with narrow, elongated channels guides the electrochemical deposition of metal ions to form nanowires. Commonly used templates, such as anodic aluminum oxide (AAO), contain densely arranged nanopores that enable the fabrication of compact nanowire arrays. This “template” is what makes such a method attractive for implementing in various energy and/or electronics applications because the template itself provides mechanical robustness and serves as an electrical insulator that keeps dense nanowires separated from each other.

However, a critical limitation arises in template-assisted electrodeposition when implemented for device applications that require electrical connection at both ends of the nanowires. That is, the length uniformity of the nanowires synthesized by this method is shown to be extremely poor. When certain nanowires grow faster and emerge from the template, they expand laterally without restriction, thereby blocking neighboring pores (Fig. 1a). Consequently, only a small fraction,

typically well below 1%, of the nanowires achieve full connection between both ends of the template.<sup>7</sup>

One major reason for this behavior is the non-uniform ion transport near and within the long, narrow nanopores. Since the size of individual pores is always irregular and dispersed,<sup>8,9</sup> local mass transfer and resulting concentration gradients near the growth front are seldom uniform.<sup>10,11</sup> This effect is more pronounced in disordered commercial AAO membranes such as Anodisc, which are convenient to use but irregular in pore size (otherwise, fabricating home-made AAO membranes involves tedious fabrication steps and elaborate effort). Also, the non-uniform ion transport becomes more prominent in the presence of an electrolyte with a low concentration used for nanowire growth, which is inevitable for particular circumstances

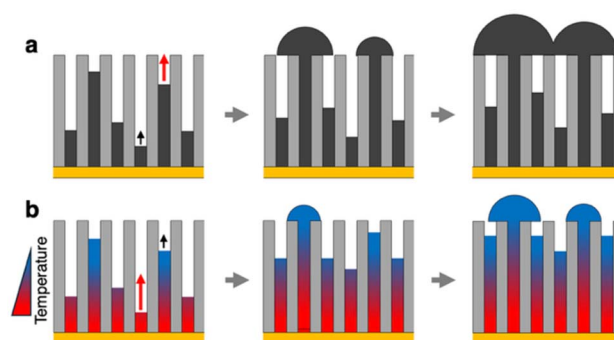


**Fig. 1** Self-controlled growth of nanowires via thermal gradients. (a) Unstable growth of nanowires in template-assisted electrodeposition. (b) Suppression of growth instability by introducing temperature gradients across the nanoporous template, resulting in more uniform nanowire growth.

<sup>a</sup>Department of Mechanical Engineering, Seoul National University of Science and Technology, 01811, Seoul, The Republic of Korea. E-mail: kimmbs@seoultech.ac.kr

<sup>b</sup>Department of Mechanical and Aerospace Engineering, University at Buffalo, The State University of New York, Buffalo, NY, 14260, USA

<sup>c</sup>Department of Mechanical Engineering, Yonsei University, 03722, Seoul, The Republic of Korea. E-mail: hhcho@yonsei.ac.kr


that require a low concentration of metallic salts ( $<0.1$  M), such as synthesizing bismuth<sup>12</sup> or bismuth compound structures.<sup>13</sup>

Moreover, this non-uniform nanowire growth is inherently an unstable process where the non-uniform ion transport accelerates the uneven growth of the nanowires.<sup>10,14</sup> That is, ions transported through pores containing longer nanowires can more easily reach the growth front because the remaining pore length is shorter; this leads to accelerated nanowire growth for the longer nanowires compared to the shorter ones.

To date, several efforts have been devoted to mitigating this non-uniform ion transport and enhancing nanowire length uniformity, for instance, by employing pulsed electrodeposition,<sup>15–18</sup> lowering the deposition temperature,<sup>15,19</sup> or modulating surface conduction.<sup>20</sup> Although these approaches have been shown to be fairly effective in enhancing nanowire length uniformity, they are based solely on suppressing the overall transport and reaction rate, which fails to prevent the positive-feedback process.

Previously, we reported that imposing temperature gradients across nanoporous templates could suppress growth instability,<sup>10</sup> which was later studied theoretically by others.<sup>14,21</sup> In this work, we present a comprehensive investigation of temperature-gradient-driven nanowire electrodeposition and demonstrate that the growth instability can be experimentally controlled, resulting in enhanced nanowire growth. The difference in the tip temperature of individual nanowires caused by the fin effect triggers a self-controlled growth mechanism that regulates their own growth rate and enhances overall length uniformity. Even with a highly disordered nanowire template (Anodisc) and a low electrolyte concentration (20 mM), we show that it is possible to enhance nanowire length uniformity by more than 40% compared to nanowires grown under uniform temperature conditions.

## 2. Results and discussion

The concept of self-controlled nanowire growth *via* temperature gradients is shown in Fig. 1b. When the temperature of the bottom side (seed layer) of the template is high, and the temperature of the electrolyte is maintained at a low temperature, the temperature at the tips (growth front) of the nanowires should be different depending on the length of the nanowires because temperature gradient is drawn along the nanowires by fin effect. For instance, the tip temperature of a long nanowire should be low whereas that of a short nanowire should be high, which implies that the electrochemical reaction at the short nanowire should be much faster compared to the long nanowire because the electrochemical reaction is highly dependent on the temperature, which follows the Arrhenius relation. Therefore, shorter nanowires should grow faster than longer nanowires, enabling self-controlled growth for enhancing the length uniformity.

Therefore, to induce local temperature gradients along the nanowires during electrodeposition, we built a reaction cell that includes an ambient temperature control unit along with a local heating unit (Fig. 2). The ambient temperature of the electrolyte was controlled by external water jacket that circulates through

a constant temperature bath (Fig. 2a). Local heating along the nanowires was enabled by a microfabricated heater/sensor device (Fig. 2b and c). An indium tin oxide (ITO) heater, along with a platinum resistance temperature detector (RTD), deposited on a silicon substrate induces and measures the temperature gradient (Fig. 2c). On the backside, copper foil was deposited as a working electrode. Here, nanowire template (Anodisc, average pore diameter = 320 nm),<sup>8</sup> which is sputtered with 300 nm-thick copper layer on one side, was placed. To prevent unwanted heating of the electrolyte, the device was sealed with epoxy, leaving only the growth area exposed. Also, the electrolyte was vigorously stirred to ensure a uniform bath temperature.

In order for a temperature gradient to be drawn along the nanowires under such a short length, thermal conductivity of the nanowires as well as AAO must be as low as possible. We have chosen bismuth for this purpose due to the low thermal conductivity ( $0.8 \text{ W m}^{-1} \text{ K}$  at 300 K for electrodeposited bismuth nanowires.<sup>22</sup>) Also, the thermal conductivity of Anodisc is known as about  $0.9 \text{ W m}^{-1} \text{ K}$  at 300 K.<sup>23</sup> Such low thermal conductivity values of bismuth nanowires and AAO are expected to increase the temperature gradient along the nanowires. Moreover, the similar thermal conductivities of the two

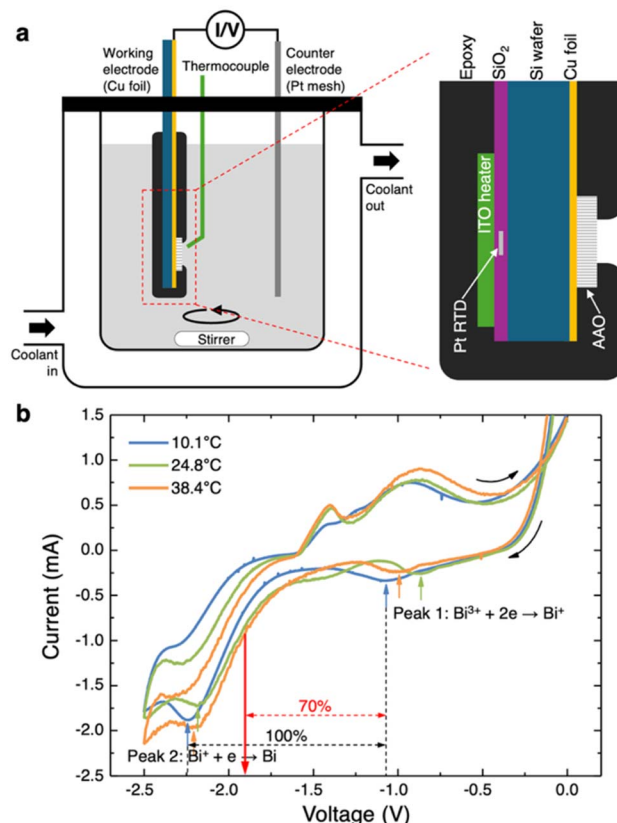


Fig. 2 (a) An electrodeposition cell capable of achieving local temperature gradients across nanoporous anodic aluminum oxide (AAO) template. (b) Cyclic voltammetry for bismuth under various bath temperatures. Red arrow indicates assigned overpotential, which is 70% between the two reduction peaks (peak 1 and 2).



materials will minimize any significant thermal crosstalk between the neighboring nanowires, thus maintaining the individual temperature of the nanowires mostly along their length.

As our goal is to self-regulate the electrochemical reaction rates across the whole nanowire by inducing a temperature difference, other factors besides temperature that influence the reaction rate should be strictly regulated. To this end, a rigorous control of the overpotential is critical since a slight difference in the overpotential leads to an unfair comparison across the experiment cases. Therefore, rather than using a reference electrode, we applied a certain overpotential that was individually determined from cyclic voltammetry prior to potentiostatic electrodeposition. In detail, we have observed two reduction peaks for the bismuth salt, which are  $\text{Bi}^{3+}$  to  $\text{Bi}^+$  reduction near  $-1$  V (peak 1) and  $\text{Bi}^+$  to  $\text{Bi}$  reduction near  $-2.3$  V (peak 2),<sup>12</sup> as shown in Fig. 2. Between these two particular events, we have chosen a certain overpotential for the electrodeposition of bismuth, which is 70% point closer to peak 2 between the two reduction peaks (indicated as red arrow in Fig. 3). This particular value was chosen as an optimal value for the electrodeposition because if the overpotential was higher than this value, *i.e.* closer to peak 2, the growth of the nanowires was too fast so that the self-controlled growth could not be

observed whereas if the overpotential was lower than this value, *i.e.* closer to peak 1, growth of the nanowires did not initiate due to the narrow potential window for electrochemical reduction to occur.

The results for the length uniformity in various experimental conditions are presented in Fig. 3. Fig. 3a–c show the back-scattered scanning electron microscope (SEM) images for the cross-sections of the nanowire-embedded AAO templates grown at various bottom surface temperatures  $T_s$  while the bulk electrolyte temperature  $T_b$  is fixed at  $T_b = 10^\circ\text{C}$ . Bright and dark contrasts in SEM images correspond to bismuth and alumina, respectively. When synthesized at  $10^\circ\text{C}$  without any local heating ( $T_s = T_b = 10^\circ\text{C}$ ), it is shown that only a small fraction of the template is filled with nanowires. However, as  $T_s$  increases due to the local heating, the length of the nanowires occupying the AAO template increases along with more image contrast between the nanowires and AAO, indicating more bismuth nanowires. The quantitative length uniformity, which is presented in Fig. 3d, was estimated as the ratio of the average length of the fully grown nanowires to the thickness of the nanowire template, where the error bars represent the degree of fluctuation of the overall length of nanowires. It is shown that the average length uniformity increases as  $T_s$  is increased up to a certain point (red triangles). At  $T_s = 28.8^\circ\text{C}$ , the length uniformity reaches up to 49.4%, which is 40% enhancement compared to the baseline experiment. After  $T_s = 30^\circ\text{C}$ , the length uniformity dramatically decreases.

Unambiguously, this length uniformity enhancement is not attributed to the overall temperature change, but due to the temperature gradient, as confirmed by further experiments in which we have carried out; electrodeposition of the nanowires without local heating under various uniform temperatures. Blue circles in Fig. 3d represent the length uniformity of the nanowires under various uniform electrolyte temperatures without local heating. The results reveal that without local heating, as the overall temperature is increased the length uniformity of the nanowires is slightly decreased, which is in agreement with previous reports,<sup>15,19</sup> and the results clearly deviate from the local heating results (red triangles). Therefore, it is evident that the temperature gradient plays a critical role in enhancing the length uniformity during electrodeposition.

By analyzing chronoamperometric curves during electrodeposition, it is possible to further elucidate the relationship between length uniformity and temperature gradient. Fig. 4a shows a typical chronoamperometric curve for nanowire electrodeposition. In brief, the nanowires begin to grow along the nanopores where the deposition current shows relatively steady behavior (stage (i)). As some fully grown nanowires begin to grow outside the template and form hemispherical caps, the deposition current rises due to the enlarged surface area (stage (ii)). The caps block nearby pores, which hinders the growth of nearby nanowires. The caps eventually form a continuous film, such that the deposition current levels off again (stage (iii)). These stages are separated by two particular points of inflection, which are denoted as  $t_1$  and  $t_2$ . Reflecting this curve to the length uniformity, an ideal curve that exhibits a perfect length uniformity should resemble a step-function where the

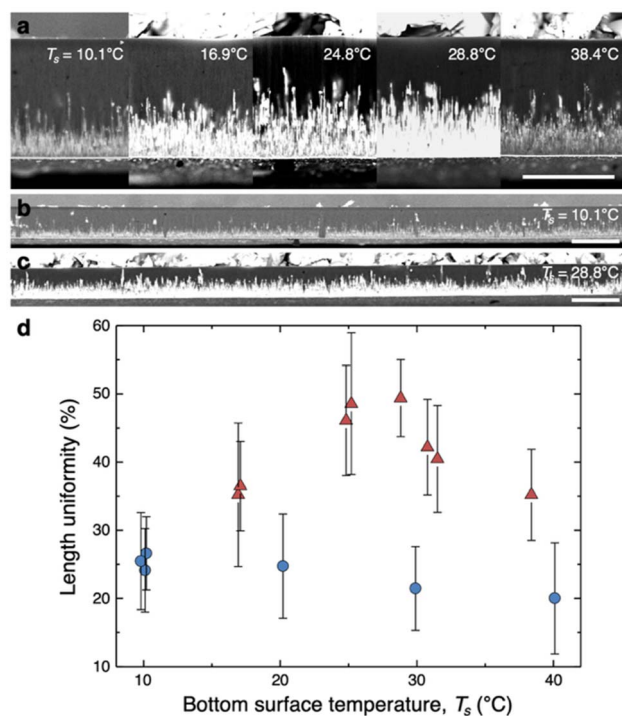
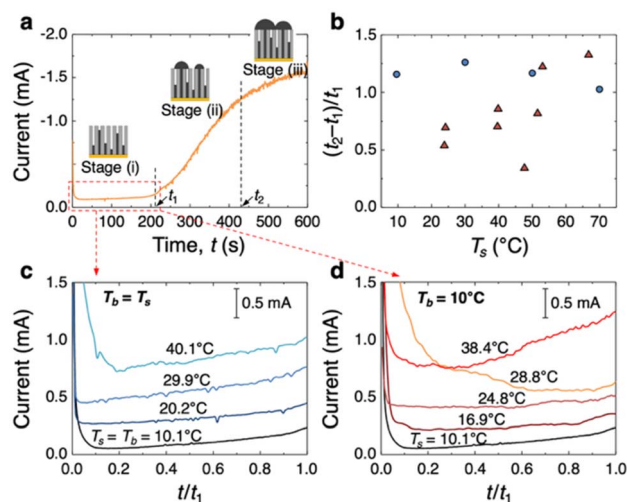


Fig. 3 Length uniformity of nanowires under various temperatures. (a) Back-scattered SEM images of cross-sections of nanowire-embedded AAO templates under various bottom surface temperatures,  $T_s$ . (b and c) Zoomed-out SEM images when  $T_s$  is (c)  $10.1^\circ\text{C}$  and (d)  $28.8^\circ\text{C}$ . (d) Average length uniformity of nanowires grown at different  $T_s$ . Blue circles indicate experiments under uniform temperature ( $T_s = T_b$ ), whereas red triangles indicate experiments with local heating ( $T_s > T_b$ ). Scale bars are (a)  $50\ \mu\text{m}$  and (b and c)  $100\ \mu\text{m}$ .





**Fig. 4** Chronoamperometric curves for electrodeposition of bismuth nanowire under various conditions. (a) Chronoamperometric curve for normal potentiostatic electrodeposition under uniform temperature. Insets illustrate morphological behavior at each growth stage. (b)  $t_2$  to  $t_1$  ratios for various  $T_s$ . Blue circles indicate experiments under uniform temperature ( $T_s = T_b$ ), whereas red triangles indicate experiments with local heating ( $T_s > T_b$ ). (c) and (d) Chronoamperometric curves at stage (i) for various  $T_s$  (c) without and (d) with local heating. Time is normalized by  $t_1$ .

overgrowth is instantaneous ( $t_1 = t_2$ ). In this sense, growth behavior during the overgrowth period (stage (ii)) should be closely related to the length uniformity. Thus, we analyze the ratio between time taken in stage (i) ( $t_1$ ) and (ii) ( $t_2 - t_1$ ) to compare across different time scales for various experiments, as presented in Fig. 5b. For experiments without local heating (blue circles),  $(t_2 - t_1)/t_1$  is near unity due to poor length uniformity, and is insensitive to the temperature change, implying that this is a universal trend. However,  $(t_2 - t_1)/t_1$  for experiments with local heating (red triangles) are located far below unity, indicating improved simultaneous overgrowth of nanowires. Also, this value is sensitive to  $T_s$ , which tends to increase with  $T_s$  and exceeds unity when  $T_s > 30$  °C. Therefore, we confirm that local heating results in more concurrent growth of nanowires with enhanced length uniformity. However, a critical question remains: Is the temperature gradient responsible for suppressing the non-uniform growth and inducing self-controlled growth?

By taking a closer look at stage (i) in Fig. 4a, we were able to find direct evidence for the answer. For normal electrodeposition of nanowires under uniform temperature, the deposition current gradually increases because the nanowires grow, the ion concentration gradient and the electric field increase, leading to faster, unstable nanowire growth. As we examine the experiments without local heating in Fig. 5c, it is shown that the deposition current increases as the electrodeposition proceeds, and the degree of such increase becomes more prominent as the temperature increases. This implies accelerated growth instability at higher temperatures, leading to poor length uniformity.

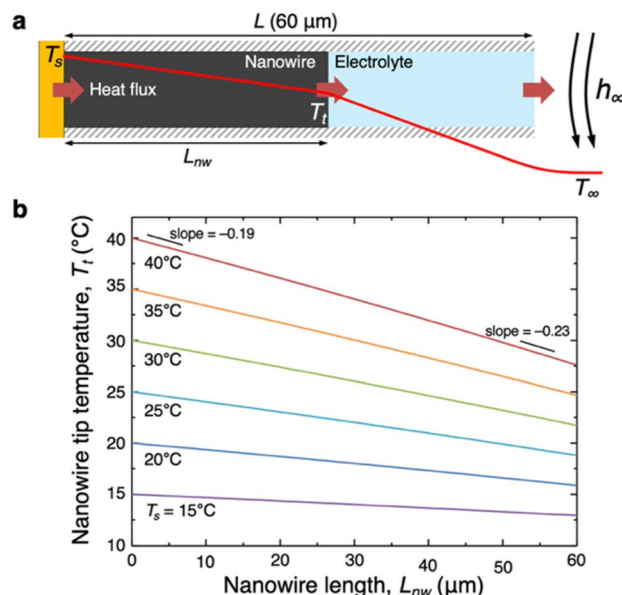


**Fig. 5** Heat transfer analysis of a nanowire inside a pore. (a) Schematic of the cross-section of the nanowire-embedded nanopore. Red curve represents the expected temperature profile along the nanopore. (b) Nanowire tip temperature  $T_i$  for different nanowire length  $L_{nw}$  under various  $T_s$ .

In contrast, when temperature gradients are formed along the nanowires due to local heating, distinct behaviors are observed (Fig. 4d). As  $T_s$  increases, the increase in the deposition current tends to be suppressed, and it even shows a decreasing behavior at 28.8 °C, which is the case for the best length uniformity. Then, as the temperature further increases, the deposition current again tends to increase. These behaviors cannot be explained by the overall temperature rise because electrochemical reactions are faster at higher overall temperatures. We believe that this is direct evidence for the self-controlled growth enabled by temperature gradients.

The fin effect may have triggered this self-controlled growth, where the deposition current actually decreases as the nanowires grow. At the early stage, the length deviation of the nanowires is not significant so that the tip temperature of the nanowires (growth front) should be similar among the nanowires. However, the unstable growth leads to increased deviation in the nanowire length as well as the tip temperature. This triggers self-controlled growth where the electrochemical reaction of longer nanowires is expected to be slower than shorter ones. Recalling that the deposition current increase in stage (i) is mainly due to the accelerated growth of the longer nanowires, the deposition current is expected to decrease as the electrodeposition proceeds when the tip temperature deviation is at maximum, which we observe in  $T_s = 28.8$  °C case.

The unstable growth behavior that reemerges at elevated temperature ( $T_s > 30$  °C) is ambiguous. One possible reason is that the suppressed growth due to the fin effect is overcome by increased ion diffusion along the pore channels due to the increased overall temperature. Therefore, the fin effect is unable to suppress the growth instability at higher temperatures. In



a physical sense, this is somewhat in conjunction with what we have previously mentioned where a large overpotential cannot induce self-controlled growth behavior due to fast nanowire growth. Nevertheless, we confirm that, to a certain degree ( $T_s < 28.8\text{ }^\circ\text{C}$ ), the temperature gradient evidently induces self-controlled growth that leads to enhanced length uniformity.

To evaluate how temperature variations influence nanowire growth, we perform a heat transfer analysis to calculate the temperature profiles along the nanowires and assess the resulting changes in ion diffusion. As discussed earlier, the comparable thermal conductivities of bismuth nanowires and AAO permit us to approximate the heat transport as one-dimensional (1-D) along the nanowire axis. Under this 1-D assumption, the thermal pathway and the corresponding temperature profile are depicted in Fig. 5a. Since only conduction occurs on the electrolyte inside the pores of the template due to the high aspect ratio of the pores,<sup>24</sup> the nanowire-electrolyte system can be treated as a composite fin with convective heat loss at the end. The temperature at the nanowire tip,  $T_t$ , can be expressed as

$$T_t = \frac{h_\infty k_e L_{\text{nw}} T_b + h_\infty k_{\text{nw}} (L - L_{\text{nw}}) T_s + k_e k_{\text{nw}} T_\infty}{h_\infty k_e L_{\text{nw}} + h_\infty k_{\text{nw}} (L - L_{\text{nw}}) + k_e k_{\text{nw}}}, \quad (1)$$

where  $h_\infty$  is the convective heat transfer coefficient due to stirring ( $8500\text{ W m}^{-2}\text{ K}^{-1}$  at 300 rpm),<sup>25</sup>  $k_e$  is the thermal conductivity of the electrolyte ( $0.6\text{ W m}^{-1}\text{ K}$  at 300 K for water),  $k_{\text{nw}}$  is the thermal conductivity of the nanowire ( $0.8\text{ W m}^{-1}\text{ K}$  at 300 K for electrodeposited bismuth nanowire with a diameter of 250 nm),<sup>26</sup>  $L$  is the length of the nanowire template (60  $\mu\text{m}$ ), and  $L_{\text{nw}}$  is the length of the nanowire.

Fig. 5b presents the calculated tip temperature  $T_t$  as a function of nanowire length  $L_{\text{nw}}$  for several  $T_s$ , based on eqn (1). The results suggest that the temperature difference between long and short nanowires is significant, arising from the fin effect due to the low thermal conductivity of bismuth, and that this difference amplifies as the  $T_s$  increases. For instance, when  $T_s = 30\text{ }^\circ\text{C}$ ,  $T_t$  is  $23.2\text{ }^\circ\text{C}$  for a 50  $\mu\text{m}$ -long nanowire and  $24.6\text{ }^\circ\text{C}$  for a 40  $\mu\text{m}$ -long nanowire. This modest temperature difference of  $1.4\text{ }^\circ\text{C}$  produces a 7.0% change in the diffusion coefficient (estimated from the Stokes–Einstein and Arrhenius relations, with the activation energy extracted as 0.34 eV from growth rate *versus* temperature data). These results indicate that a substantial temperature gradient can indeed be established along nanowires to induce self-regulated growth. Furthermore, Fig. 5b shows that the slope of the curves becomes steeper with longer nanowires. This suggests that the self-regulation due to thermal gradients should intensify in the later stages of electrodeposition, potentially explaining the observed reduction in the deposition current (Fig. 4d).

### 3. Conclusions

In summary, we have reported a strategy to suppress growth instabilities and achieve self-regulated electrodeposition of bismuth nanowires, leading to improved length uniformity. Electrochemical measurements and heat transfer analysis revealed that the fin effect generates temperature differences

along nanowires, inducing self-controlled growth by modulating local transport rates. This mechanism not only improves uniformity but also suggests that thermally driven self-regulation could extend to other materials and synthesis methods governed by diffusion-limited processes.<sup>27,28</sup>

### Conflicts of interest

There are no conflicts to declare.

### Data availability

The data presented in the study are included in the article; further inquiries can be directed to the corresponding author.

### Acknowledgements

This study was financially supported by Seoul National University of Science and Technology.

### References

- 1 C. Jia, Z. Lin, Y. Huang and X. Duan, *Chem. Rev.*, 2019, **119**, 9074–9135.
- 2 A. I. Hochbaum, R. Chen, R. D. Delgado, W. Liang, E. C. Garnett, M. Najarian, A. Majumdar and P. Yang, *Nature*, 2008, **451**, 163–167.
- 3 G. Zhou, L. Xu, G. Hu, L. Mai and Y. Cui, *Chem. Rev.*, 2019, **119**, 11042–11109.
- 4 S. Shin, G. Choi, B. Rallabandi, D. Lee, D. I. Shim, B. S. Kim, K. M. Kim and H. H. Cho, *Nano Lett.*, 2018, **18**, 6392–6396.
- 5 G. Cao and D. Liu, *Adv. Colloid Interface Sci.*, 2008, **136**, 45–64.
- 6 A. Davydov and V. Volgin, *Russ. J. Electrochem.*, 2016, **52**, 806–831.
- 7 S. Shin and H. H. Cho, *Electrochim. Acta*, 2014, **117**, 120–126.
- 8 S. Shin, B. S. Kim, K. M. Kim, B. H. Kong, H. K. Cho and H. H. Cho, *J. Mater. Chem.*, 2011, **21**, 17967–17971.
- 9 S. Shin, B. S. Kim, J. Song, H. Lee and H. H. Cho, *Lab Chip*, 2012, **12**, 2568–2574.
- 10 S. Shin, T. T. Al-Housseiny, B. S. Kim, H. H. Cho and H. A. Stone, *Nano Lett.*, 2014, **14**, 4395–4399.
- 11 D. Bogachev, T. Kabanova and A. Davydov, *J. Solid State Electrochem.*, 2025, **29**, 1309–1340.
- 12 S. Holvoet, P. Horny, S. Turgeon, P. Chevallier, J.-J. Pireaux and D. Mantovani, *Electrochim. Acta*, 2010, **55**, 1042–1050.
- 13 Y. Miyazaki and T. Kajitani, *J. Cryst. Growth*, 2001, **229**, 542–546.
- 14 A. Fang and M. Haataja, *J. Electrochem. Soc.*, 2017, **164**, D875.
- 15 L. Trahey, C. R. Becker and A. M. Stacy, *Nano Lett.*, 2007, **7**, 2535–2539.
- 16 J. Lee, S. Farhangfar, J. Lee, L. Cagnon, R. Scholz, U. Gösele and K. Nielsch, *Nanotechnology*, 2008, **19**, 365701.
- 17 K. Nielsch, F. Müller, A.-P. Li and U. Gösele, *Adv. Mater.*, 2000, **12**, 582–586.
- 18 A. Sharma, S. Bhattacharya, S. Das and K. Das, *Surf. Eng.*, 2016, **32**, 378–384.



- 19 S. Shin, B. H. Kong, B. S. Kim, K. M. Kim, H. K. Cho and H. H. Cho, *Nanoscale Res. Lett.*, 2011, **6**, 467.
- 20 J.-H. Han, E. Khoo, P. Bai and M. Z. Bazant, *Sci. Rep.*, 2014, **4**, 7056.
- 21 D. A. Bograchev and A. D. Davydov, *Electrochim. Acta*, 2019, **296**, 1049–1054.
- 22 A. L. Moore, M. T. Pettes, F. Zhou and L. Shi, *J. Appl. Phys.*, 2009, **106**, 034310.
- 23 D.-A. Borca-Tasciuc and G. Chen, *J. Appl. Phys.*, 2005, **97**, 084303.
- 24 K. Kim, M. Kim and S. M. Cho, *Mater. Chem. Phys.*, 2006, **96**, 278–282.
- 25 T. H. Chilton, T. B. Drew and R. H. Jebens, *Ind. Eng. Chem.*, 1944, **36**, 510–516.
- 26 J. H. Seol, A. L. Moore, S. K. Saha, F. Zhou, L. Shi, Q. L. Ye, R. Scheffler, N. Mingo and T. Yamada, *J. Appl. Phys.*, 2007, **101**, 023706.
- 27 R. S. Wagner and W. C. Ellis, *Appl. Phys. Lett.*, 1964, **4**, 89–90.
- 28 B. Liu and H. C. Zeng, *J. Am. Chem. Soc.*, 2003, **125**, 4430–4431.

